Energy Storage Materials 6 (2017) 119–124

Contents lists available at ScienceDirect

Energy Storage Materials

journal homepage: www.elsevier.com/locate/ensm

Stabilized Li_3N for efficient battery cathode prelithiation

Yongming Sun[a,1], Yanbin Li[a,1], Jie Sun[a], Yuzhang Li[a], Allen Pei[a], Yi Cui[a,b,*]

[a] Department of Materials Science and Engineering, Stanford University, Stanford, CA 94305, United States
[b] Stanford Institute for Materials and Energy Sciences, SLAC National Accelerator Laboratory, 2575 Sand Hill Road, Menlo Park, CA 94025, United States

ARTICLE INFO

Keywords:
Li_3N
Cathode prelithiation
Surface passivation
Stability
High capacity

ABSTRACT

Li_3N can deliver more than 10 times the theoretical capacity of existing cathode materials and can serve as an excellent cathode prelithiation additive to offset the initial lithium loss in lithium-ion batteries. However, Li_3N has intrinsic problems of poor environmental and chemical stability in battery electrode processing environments due to its reactivity with moisture in ambient conditions and incompatibility with solvents used for battery slurry mixing. Herein, we report a facile route to prepare a surface-passivated Li_3N material by the reaction of lithium metal with nitrogen followed by an annealing process. A dense surface passivation layer consisting of crystalline Li_2O and Li_2CO_3 isolates the active composition of materials from air and thus enables good stability of Li_3N particles in ambient conditions. The as-prepared Li_3N powder is processable by slurry coating for electrode fabrication using a low-polarity solvent. The Li_3N is verified to work as a secondary lithium source to offset the initial capacity loss at the anode using a Li_3N/graphite cell configuration. A high "donor" lithium-ion specific capacity of 1761 mAh/g is achieved for a pristine Li_3N electrode. When Li_3N is included into cathodes, including $LiCoO_2$ (LCO), $LiNi_{0.6}Co_{0.2}Mn_{0.2}O_2$ (NCM) and $LiFePO_4$ (LFP), the hybrid electrodes can be baked and calendared in ambient conditions, and, as expected, high prelithiation efficiency is achieved. As a typical example, with a 2.5% Li_3N additive, a LCO electrode delivers a 51 mAh/g higher capacity than that of the pristine LCO electrode in the first charge process and shows stable cycling behavior. The good stability and high prelithiation efficiency of the Li_3N powder enable its potential application in high-performance lithium-ion batteries.

1. Introduction

There is unrelenting demand for rechargeable lithium-ion batteries (LIBs) with higher energy density to address the ever-increasing energy needs of modern society for wide applications such as extended-range electric vehicles and grid-scale storage [1–4]. The electrodes of batteries largely decide their lithium storage capacity and energy density [5,6]. In existing lithium-ion technology, lithium is provided by lithium-intercalated cathode materials, such as $LiCoO_2$ (LCO), $LiNi_{0.6}Co_{0.2}Mn_{0.2}O_2$ (NCM) and $LiFePO_4$ (LFP). Graphite has been as the most commonly used commercial anode material for LIBs since 1991 due to its high reversibility and low cost [7]. On the other hand, various alternative high-capacity anode materials such as silicon, with a theoretical capacity more than ten times that of graphite [8,9], have been well studied and have already shown promise in potential applications. The formation of a solid electrolyte interphase (SEI) layer on the anode surfaces is a critical process that occurs prior to regular battery operations and consumes a significant amount of lithium, irreversibly reducing the overall capacity of batteries. Graphite anodes exhibit an irreversible capacity loss of 5–10% from the initial battery charging process [10–14], while for high-capacity anode materials, the first-cycle lithium loss is even higher (*e.g.*, 15–35% for Si) [15]. Such lithium loss in the so-called "formation process" appreciably reduces the energy density of LIBs.

Electrochemical prelithiation is an effective route to solve the issue of initial lithium loss in LIBs; however, it needs an extra process of electrochemical cell building [16]. To improve the overall energy density of LIBs, it is vitally important to pre-store lithium into electrodes to compensate the initial lithium loss by using high-capacity, low-cost, environment/dry air stable prelithiation materials. Currently, a wide range of prelithiation materials have been investigated, including anode and cathode prelithiation additives. Typical anode prelithiation materials are stabilized lithium metal [17,18] and lithium silicide powder [19–21]. Due to the high specific capacities of these anode additives (> 2000 mAh/g), the initial lithium loss of LIBs can be offset with just a small amount of additives. However, due to their low potential and high chemical reactivity, these high-capacity anode prelithiation additives have compatibility issues with common solvents,

* Corresponding author at: Department of Materials Science and Engineering, Stanford University, Stanford, CA 94305, United States.
E-mail address: yicui@stanford.edu (Y. Cui).
[1] These authors contributed equally to this work.

http://dx.doi.org/10.1016/j.ensm.2016.10.004
Received 22 August 2016; Received in revised form 10 October 2016; Accepted 10 October 2016
Available online 11 October 2016

ambient environments and thermal processing procedures involved in existing battery fabrication conditions. On the other hand, cathode prelithiation materials possess higher potentials and better chemical stability. In some early work, Li-rich compounds have been explored, such as Li_6CoO_4, Li_2NiO_2, and Li_2MoO_3 [22–25]. However, their lithium-ion donating capacities are limited (~300 mAh/g). Recently, we demonstrated that conversion reaction based nanocomposites (e.g., Li_2O/metal, LiF/metal and Li_2S/metal composites) could be attractive cathode prelithiation materials with high lithium-ion donating capacities in the range of 500–700 mAh/g, good stability and compatibility with existing battery processing conditions [26–28].

Binary lithium compounds (*e.g.*, Li_2O, LiF and Li_3N) have much higher theoretical capacities than that of Li-rich compounds and other sacrificial lithium salts [29]. Among them, Li_3N is an attractive cathode prelithiation material for LIBs, considering its high theoretical specific capacity (2309 mAh/g based on the reaction formula: $2Li_3N \rightarrow 6Li^+ + 6e^- + N_2$) and low theoretical decomposition potential (~0.44 V *vs.* Li^+/Li) [30]. A large amount of Li can be extracted from Li_3N during the "formation process" of batteries to offset the initial lithium loss. Very recently, the potential application of Li_3N as a cathode additive for $LiCoO_2$ (LCO) cathodes was investigated by blending LCO powder with ground commercial Li_3N powder (Alfa Aesar) and coating ground commercial Li_3N powder on top of pre-prepared LCO electrodes without using any solvent in an argon-filled glovebox [31]. In order to take advantage of the high prelithiation capacity of Li_3N, two challenges must be overcome: (i) Pure Li_3N has high chemical reactivity with moisture in ambient atmosphere; (ii) Li_3N is not compatible with the widely used N-methyl-2-pyrrolidone (NMP) solvent in conventional slurry casting processes due to its high reactivity [31]. These two challenges make it difficult for Li_3N to survive multiple processing steps in battery electrode fabrication, such as exposure to air, slurry mixing and baking, and electrode calendaring in ambient/dry air conditions. Therefore, it is highly desirable to design Li_3N with improved stability, and explore suitable slurry manufacturing processes.

We have previously shown that the stability of lithium silicide anode prelithiation reagents can be improved through protection by either a Li_2O shell [20] or a passivation layer consisting of LiF and lithium alkylcarbonate [19]. Very recently, we have reported that crystalline Li_2O matrix enables excellent stability of Li*x*Si in ambient air with 40% relative humidity [21]. We believe that a similar passivation layer of crystalline Li_2O and/or other lithium compounds can help to improve the chemical and environmental stability of Li_3N. Herein, we report a surface-passivated Li_3N material made through annealing fresh Li_3N in a nitrogen-filled glovebox with trace oxygen species. It is found that the reactivity of the Li_3N is suppressed under ambient conditions after the surface passivation by a dense layer consisting of crystalline Li_2O and Li_2CO_3. When a small amount of such Li_3N powder was included into various cathodes (e.g., LCO, NCM and LFP) using slurry baking and electrode calendaring operations in ambient conditions, lithium was easily extracted from Li_3N during the initial charge process and high prelithiation efficiency was achieved.

2. Materials and methods

2.1. Materials synthesis

Lithium metal foil (99.9%, Alfa Aesar, 0.75 mm thick) was used as the starting material for the synthesis of Li_3N. During the synthesis, a piece of lithium metal foil (~1 g) was put in a nitrogen-filled glovebox. After 3 days, the lithium metal foil transformed into a Li_3N flake, which was further heat-treated at 200 °C for 24 h. Li_3N powder was obtained after grinding. To fabricate the Li_3N film on a conducting substrate, lithium metal foil was first melted at 200 °C on a Cu foil. After the nitridation in a nitrogen-filled glovebox, the Li_3N film was obtained.

2.2. Characterization

The X-ray diffraction (XRD) measurements were carried out on a panalytical X'pert diffractometer with Ni-filtered Cu Kα radiation (λ=1.5406 Å). Scanning electron microscopy (SEM) and energy-dispersive X-ray spectroscopy (EDX) of the samples were acquired on a FEI XL30 Sirion scanning electron microscope. A PHI Versa Probe 5000 system (Physical Electronics, MN) was employed for X-ray photoelectron spectroscopy (XPS) characterization. Transmission electron microscopy (TEM), high-resolution transmission electron microscopy (HRTEM) and electron energy loss spectroscopy (EELS) were performed on a FEI Titan 80–300 environmental TEM. The samples were maintained at a low temperature of ~100 K by a liquid nitrogen cryo-holder during the TEM and EELS measurements.

2.3. Electrochemical measurements

2032-type coin cells were assembled in an argon-filled glove box with concentrations of moisture and oxygen below 1.0 ppm for electrochemical characterizations using 1 M $LiPF_6$ in a mixture of ethylene carbonate (EC) and diethyl carbonate (DEC) (1:1 v/v) as the electrolyte, and a Celgard 2300 membrane as the separator. Battery performances were investigated by galvanostatic charge/discharge cycling on an Arbin Battery Cycler instrument. A VMP3 potentiostat (Bio-Logic) was employed for cyclic voltammetry (CV) measurements at a scanning rate of 0.2 mV s^{-1}. Both the Li_3N film on a Cu foil and normal Li_3N electrode fabricated by a slurry method were subjected to electrochemical measurements. To prepare the pristine Li_3N electrode, Li_3N powder (60%), carbon black (30%) and polyvinylidene fluoride (PDVF, 10%) were dispersed uniformly in tetrahydrofuran (THF) to form a slurry.

All the cathodes with the addition of Li_3N were constructed using a slurry method by mixing the Li_3N powder, cathode materials, carbon black and PVDF binder at different weight ratios in THF solvent. The slurry was cast onto an Al foil. The cathodes were baked and calendared in ambient conditions. The contents of carbon black and PVDF are both 5% in weight in $LiCoO_2$ (LCO) cathodes. The as-prepared $LiFePO_4$ (LFP) and $LiNi_{0.6}Co_{0.2}Mn_{0.2}O_2$ (NCM) cathodes contain 10% carbon black and 10% PVDF. The typical mass loading of cathodes is ~4 mg/cm^2. Graphite electrodes consist of 80% graphite powder (MTI Corporation), 10% carbon black and 10% PVDF.

The lithium metal half cells of Li_3N film electrode on Cu foils were charged to 3.5 V at a current density of 0.1 mA/cm^2. Li_3N/Li and Li_3N/graphite cells were charged to 4.8/4.5 V at a current density of 30 mA/g. The galvanostatic charge/discharge measurement of LCO and NCM/Li metal half cells was carried out with the cut-off potential range of 3.2–4.5 V for the first cycle at 0.1 C and 3.2–4.3 V upon the following cycles at 0.2 C. The cut-off potential range for $LiFePO_4$/Li half metal cells is 2.5–4.5 V for the first cycle at 0.1 C and 2.5–4.2 V for the subsequent cycles at 0.2 C. The specific capacities here are caculated based on the mass of the cathode active materials. To protect samples from moisture and other reactive gases in ambient air, samples for XPS, SEM and TEM characterizations were loaded onto the sample holders, sealed in the Argon-filled glove box, and then quickly transferred into the chambers of the equipments.

3. Results and discussion

We present a simple and easily scalable synthetic route for the preparation of surface-passivated Li_3N (Fig. 1a). During the synthesis, pristine lithium metal foil was left in a nitrogen-filled glovebox with trace oxygen. The reaction between lithium metal and nitrogen gas to form Li_3N occurred spontaneously. After 3 days of exposure, the color of the lithium foil changed from white to black. As verified by XRD, the starting lithium metal was completely converted to a pure phase of *alpha*-Li_3N after the reaction with nitrogen (Fig. S1). The black Li_3N

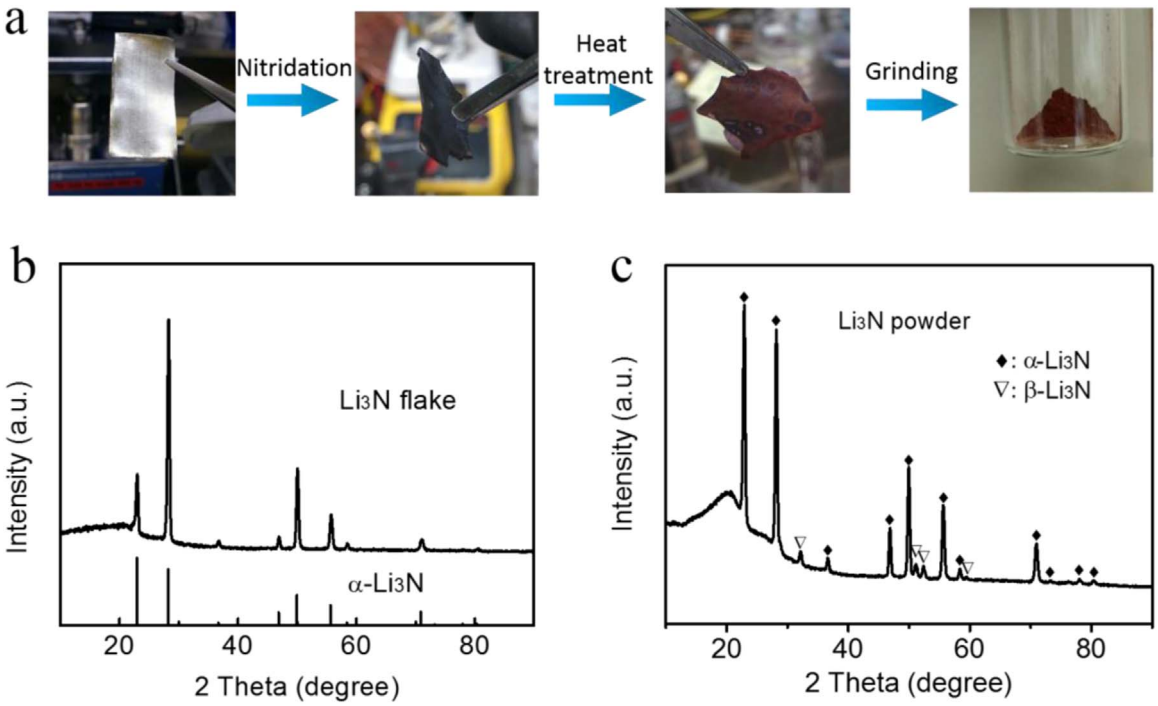

Fig. 1. Fabrication of Li_3N and XRD characterizations. (a) Synthesis of Li_3N material via nitridation of lithium metal in N_2 atmosphere and annealing processes (200 °C, 24). (b, c) XRD results of the as-prepared Li_3N flake (b) and powder after grinding (c). The XRD result shows that the as-formed Li_3N flake is pure *alpha*-phase Li_3N. After grinding, the product contains a small portion of *beta*-phase Li_3N. The XRD peaks at 21° arise from the Kapton tape.

flake turned red after an annealing process in the same environment at 200 °C for 24 h. The crystallinity and phase of the annealing products before and after mechanical grinding were also analyzed by XRD. All the diffraction peaks of the product after annealing can be readily indexed to a pure phase of *alpha*-Li_3N (Space group: P6/mmm) with a hexagonal structure (JCPDS no.: 30-0759, Fig. 1b). The XRD peaks exhibit strong intensity, indicating the high crystallinity of the as-obtained *alpha*-Li_3N. After the Li_3N flake was ground into powder, weak XRD peaks of *beta*-Li_3N were observed, due to the pressure-induced phase transformation during the mechanical grinding process (Fig. 1c) [32]. No any other impurities, such as Li_2CO_3 and Li_2O, were detected by XRD due to its limited sensitivity. The slow reaction with trace oxygen species in the glovebox during the heat treatment and grinding processes allows for the formation of a thin yet dense oxidation/passivation layer that can improve the stability of the Li_3N, making it especially suitable for battery electrode fabrication conditions in the low-humidity environment of a dry room.

XPS was carried out to investigate the surface electronic state of the as-prepared Li_3N. The binding energies were corrected by referencing the C 1 s peak to 284.5 eV. The survey XPS spectrum of a Li_3N flake verifies the chemical composition of O, N and Li (Fig. 2a). A strong O1s peak and a weak N1s peak are observed, suggesting the surface of the Li_3N flake is strongly oxidized [33]. To test the stability of the Li_3N after the annealing treatment, a Li_3N flake was exposed in ambient air with 40% relative humidity for 30 days. XRD result shows that the main phase of the sample is still *alpha*-Li_3N (Fig. 2b), although peaks of LiOH and Li_2CO_3 are detected, indicating the good stability of the surface-passivated Li_3N material. XPS investigations on the ground Li_3N powder were also performed. Fig. 2c shows the survey and high-resolution N 1 s XPS spectra of the Li_3N powder. The N peak in the survey almost disappers, suggesting the further oxidiation of Li_3N during the mechanical grinding. In contrast, when probing beyond the surface of the Li_3N powder using EDX, a strong N peak and a weak O peak are observed in the spectrum (Fig. 2d). These results indicate that only the surface of the Li_3N powder is oxidized, and the main composition of the product is Li_3N. Meanwhile, the uniform surface passivation of the as-prepared Li_3N powder is verified by the EDX mapping images (Fig. S2). In fact, the passivation layer on the surface of Li_3N particles may prevent the further oxidization of Li_3N during the material processing. The passivation layer on the Li_3N might help to suppress the penetration of moisture from ambient air deep into the entire particles, protecting the powder during handling and electrode preparation process.

The SEM images show that the Li_3N powder is composed of micrometer-size secondary particles built from interconnected particles with the size of ~300 nm (Fig. 2e, f). This hierarchical feature can help to stabilize the Li_3N in ambient conditions due to the relatively low exposed surface area of the large secondary particles. TEM, HRTEM and EELS were performed to investigate the structure and composition of the passivation layer of Li_3N particles at a low temperature of ~100 K. It is confirmed that there exists a dense layer of highly crystalline Li_2O and Li_2CO_3 on the surface of Li_3N particles (Figs. 2g and h, S3). Moreover, the surface oxidization of Li_3N particles was verified by Oxygen K-edge EELS spectrum (Fig. 2i). Similar to our previous work, the dense and highly crystalline Li_2O and Li_2CO_3 isolates the active composition of materials from air and thus enable active prelithiation materials to have enhanced stability in ambient conditions [19,21].

Electrochemical investigations were carried out on Li_3N electrodes to test the performance of the as-fabricated Li_3N powder alone. A slurry casting process was employed to fabricate the Li_3N electrodes using the surface-passivated Li_3N powder and a low-polarity tetrahydrofuran (THF) solvent. The as-prepared Li_3N electrodes exhibit a relatively high open circuit voltage (OCV) of 1.16 V and a high decomposition potential above 4 V. Impressively, a high specific capacity of 1761 mAh/g is achieved with a charge cut-off potential of 4.8 V, which is ~10 times that of current cathode materials. When the charge cut-off potential is limited to 4.5 V, the specific capacity still reaches 1163 mAh/g (Fig. 3a).This extremely high “donor” capacity demonstrates that although a small amount of capacity is sacrificed to form a passivation layer on the surface of Li_3N, the final capacity of the surface-passivated Li_3N can be improved relative to the pristine Li_3N

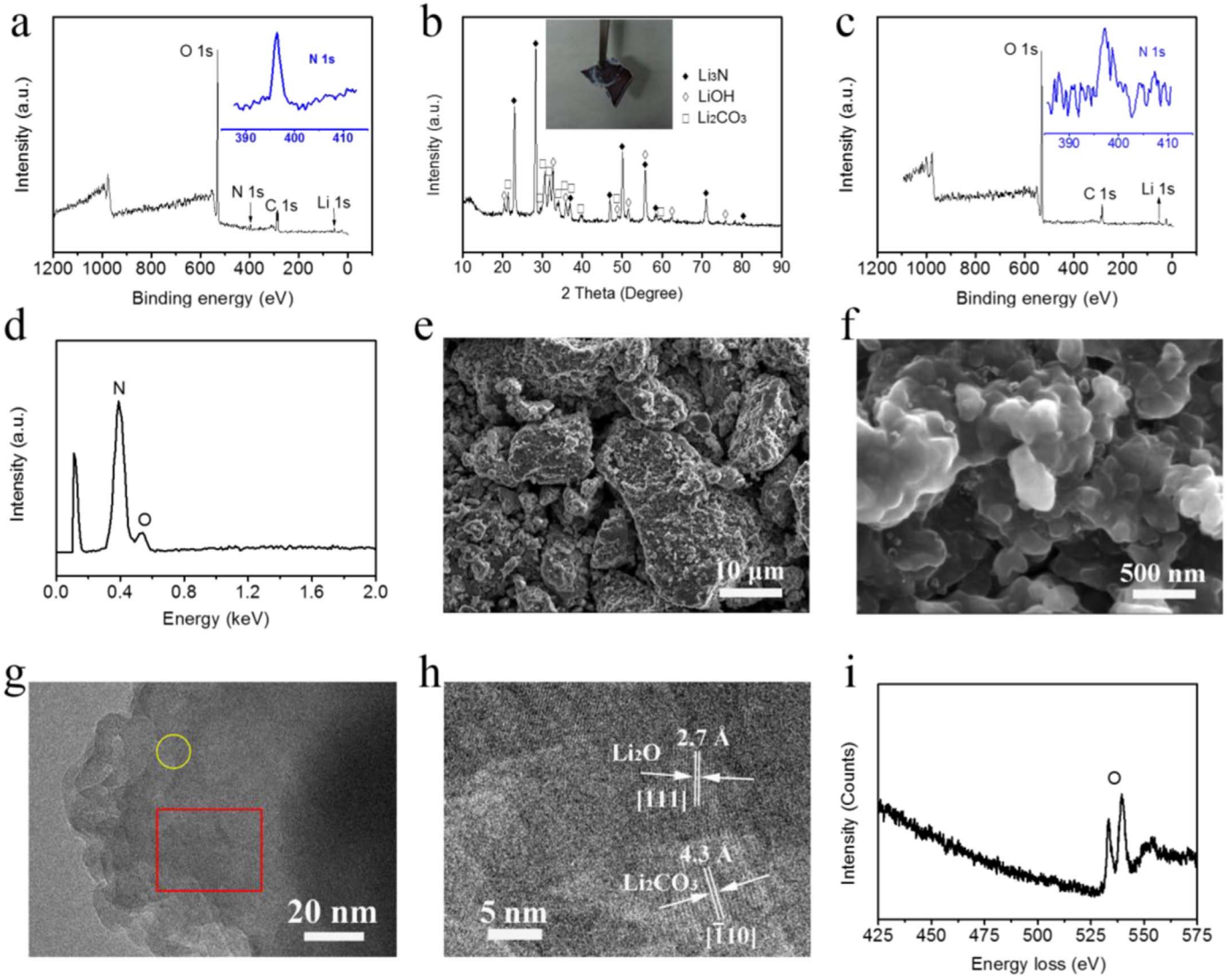

Fig. 2. Structure and stability characterizations of the as-achieved Li_3N flake and powder. (a) Survey and high-resolution N 1 s XPS spectra of a Li_3N flake, indicating that the surface of Li_3N is oxidized/passivated during the synthesis. (b) XRD result of a Li_3N flake after exposure to ambient conditions for 30 days. The main phase of the sample is still Li_3N, although LiOH and Li_2CO_3 are detected. This result indicates that the as-formed Li_3N has good envirommental stabilty. (c) Survey and high-resolution N 1 s XPS spectra of the Li_3N powder. The N peak in the survey almost disappers, suggesting the further oxidiation of Li_3N during the mechanical grinding. (d) EDX spectrum of the Li_3N powder. The strong O and weak N signals in survey XPS spectra, and the weak O and strong N signals in EDX spectrum indicate that only the surface of the Li_3N powder is oxidized, and the main composition of the product is Li_3N. (e, f) SEM images of the Li_3N powder for slurry casting process, showing that the Li_3N powder consisits of secondary Li_3N particles. (g, h) TEM image (g) taken at the the edge area of a Li_3N particle and HRTEM image (h) taken at the area labelled by a rectangle in (g). (i) Oxygen K-edge EELS spectrum collected at the yellow circle in (g). The TEM and EELS results confirm that the surface of the Li_3N particles is passivated by a dense layer consisting of crystalline Li_2O and Li_2CO_3.

[31] and its unannealed counterpart (Fig. S4) due to its better stability. Meanwhile, cyclic voltammetry (CV) measurements were also performed for Li_3N electrodes. Consistent with the potential profile, a strong oxidation peak starting from 4.30 V is clearly observed (Fig. 3b), suggesting the high decomposition potential of Li_3N electrodes. This high decomposition potential of Li_3N electrodes compared to 0.9 V in the literature study [31] may be caused by the insulating nature of the surface passivation layer on Li_3N formed during the material processing.

To investigate the effects of the passivation layer formed during the material annealing, grinding and/or slurry manufacturing processes on the decomposition potential of Li_3N, Li_3N film electrodes on a metal current collector were prepared by the nitridation of lithium metal films on Cu foils. The Li_3N particles formed on Cu foils are interconnected with each other and have sizes similar to that of the annealed and passivated Li_3N powder (200–300 nm, Fig. 3c). Without the annealing processes and other operations involved in the slurry casting processes which lead to form a passivation layer, the Li_3N film on Cu electrodes show a much lower decomposition potential (~1.15 V) than that of Li_3N electrodes fabricated using Li_3N powder with a slurry manufacturing process (Fig. 3d). Thus, surface passivation of Li_3N increases the decomposition potential, likely due to the slow kinetics of the passivation layer. A cathode prelithiation material is normally mixed with cathode active materials, binder and carbon black to fabricate cathodes. The working principle involves extracting the stored lithium from the additive on the cathode side and transferring it to the anode side to compensate the initial lithium loss. To confirm the lithium compensation effect of the as-synthesized Li_3N powder, an electrochemical cell was constructed with a Li_3N cathode and a graphite anode. Fig. 3e displays the charge potential profile of a Li_3N/graphite cell. A potential slope between 2.5 and 3 V is observed, corresponding to the formation of SEI on the graphite surface. After further charging to a higher potential, the graphite electrode is lithiated by the lithium from Li_3N, and an lithium intercalation product (LiC_{12}) is confirmed by the XRD pattern (Fig. 3f). This result indicates that during the battery charging process, the as-prepared Li_3N can be an

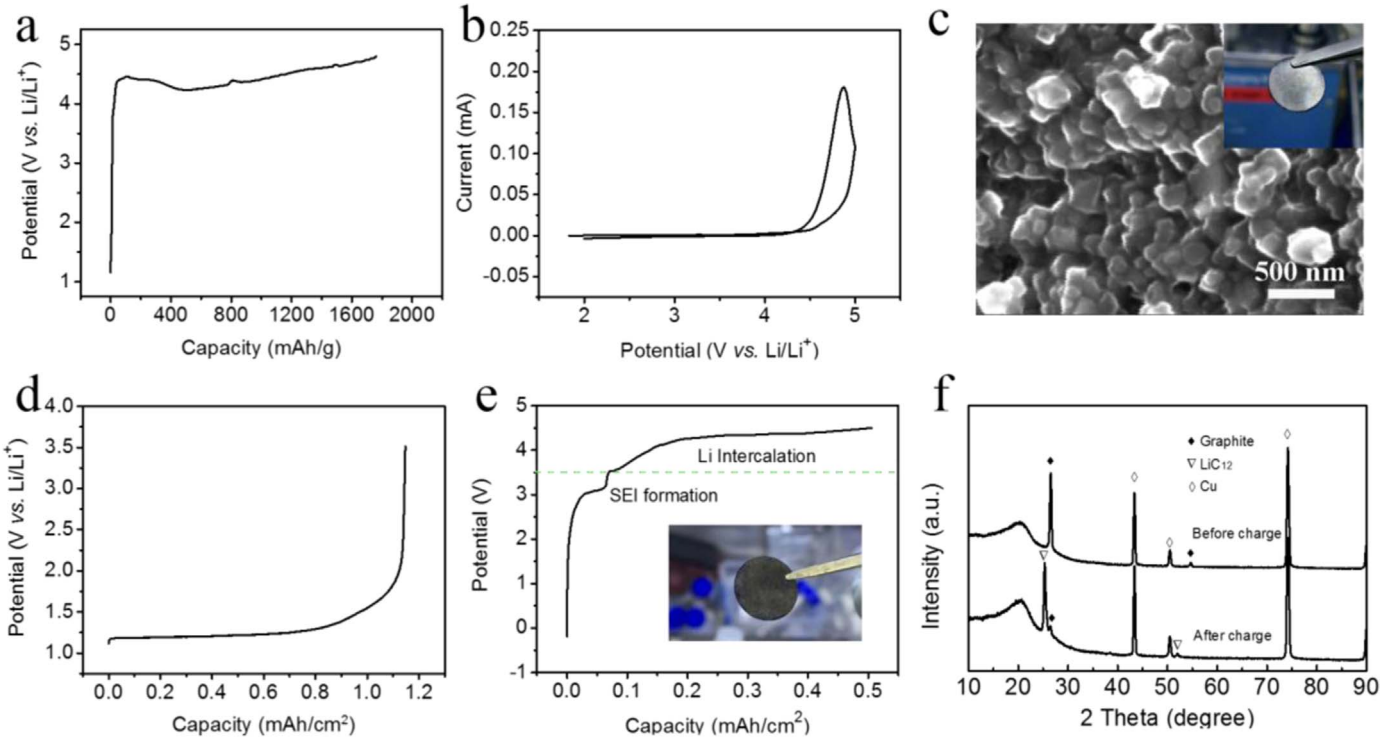

Fig. 3. Electrochemical properties of the as-prepared Li_3N electrodes. (a, b) Charge potential profile (a) and CVs (b) of a Li_3N electrode prepared by a slurry manufacturing process. (c) SEM images of a Li_3N electrode on a Cu substrate fabricated through the nitridation of a Li metal film on a Cu foil, showing that the Li_3N flim electrode consists of interconected Li_3N nanoparticles. (d) Charge potential profile of a Li_3N film electrode. (e, f) Charge potential profile of a cell with Li_3N as the cathode and graphite as the anode (e), and XRD results of the graphite anode before and after battery charging (f). The results indicate that during the battery charging process, lithium is extracted from the cathode composed of Li_3N, and the lithium loss at the anode surface caused by the formation of SEI can be compensated.

effective cathode prelithiation material to offset the lithium loss at the anode surface caused by the formation of SEI and/or other side reactions.

After comfirming the lithium compensation effect of the as-synthesized Li_3N material, we investigated the electrochemical performance of LCO cathodes with the addition of various amounts of Li_3N powder. A slurry casting process was used to prepare the hybrid cathodes so that Li_3N powder can be uniformly distributed throughout the electrodes. The electrode baking and calendaring processes were carried out in ambient atmosphere before battery assembly. The galvanostatic charge/discharge measurement of LCO cells was carried out with the cut-off potential range of 3.2–4.5 V for the first cycle (formation process) at 0.1 C to maximize the amount of lithium extracted from Li_3N, and 3.2–4.3 V upon the following cycles at 0.2 C to achieve good cycling performance. Compared with the pristine LCO electrode, the potential profile of the LCO cathode with Li_3N addtive extends above 3.8 V in the charge process, arising from the decomposition of Li_3N during charging (Fig. 4a). With the addition of 2.5% Li_3N, the initial charge capacity of the LCO cathode reaches 246 mAh/g, 51 mAh/g higher than the pristine LCO electrode. This increased capacity corresponds to 1782 mAh/g from Li_3N, indicating that high utilization of Li_3N is achieved in LCO cathodes. When 5% Li_3N is included into a LCO electrode, the cathode delivers a even higher initial charge capacity of 291 mAh/g with an extra Li-ion capacity supply of 96 mAh/g from Li_3N. Furthermore, after the initial cycle, both the LCO electrodes with and without Li_3N display similar discharge capacities (based on the mass of LCO, ~150 mAh/g) and stable cycling (Figs. 4b and S6). This good cycling performance confirms that the Li_3N additive does not have obvious negative effects on the stability of cathodes, although the decomposition of micrometer-size Li_3N produces a small amount of "holes" in the electrodes due to the evolution of nitrogen. The nitrogen gas caused by the Li_3N additive during the first cycle can be easily removed before the battery is sealed, which is accepted in a real battery system. To show the generality of using Li_3N as a prelithiation additive for various cathodes, we also prepared NCM and LFP cathodes with Li_3N additives using the same electrode fabrication procedures. As expected, their initial charge capacities increase significantly. The initial charge capacity of a NCM electrode with 2.5% Li_3N is 273 mAh/g, while a pristine NCM electrode delivers an initial charge capacity of 229 mAh/g (Fig. 4c). After adding 2.5% Li_3N in a LFP electrode, the first charge profile shows two obvious pleateaus. The first plateau is around 3.48 V with a capacity of ~170 mAh/g, while the second plateau is around 4.1 V, delivering a capacity of 62 mAh/g, corresponding to the extraction of Li from Li_3N (Fig. 4d).

4. Conclusions

In summary, surface-passivated Li_3N powder was prepared through a spontaneous chemical reaction between lithium metal and nitrogen, followed by an annealing process in a nitrogen filled glovebox with trace oxygen species. The surface passivation layer of Li_3N particles consists of dense and highly crystalline Li_2O and Li_2CO_3, which imparts good environmental stability and an increased electrochemical decomposition potential. Electrochemical extraction of lithium from a Li_3N electrode was confirmed by characterizing a cell with a Li_3N cathode and a graphite anode. The as-synthesized Li_3N exhibits a high OCV (1.16 V *vs.* Li^+/Li) and a high lithium-ion donating specific capacity of 1761 mAh/g. Electrodes using typical cathode active materials and Li_3N additives were prepared through a slurry casting process. LCO cathodes with 2.5% and 5% Li_3N additive show increased first-cycle charge capacities, 51 mAh/g and 96 mAh/g higher than that of the pristine LCO counterpart (with an initial charge capacity of 195 mAh/g), supporting the high prelithiation effectiveness of Li_3N. The stable cycling of the LCO cathodes with Li_3N additives indicate that the synthesized Li_3N has negligible effects on the cycling stability of the cathode material. Additionally, our Li_3N powder can serve as a

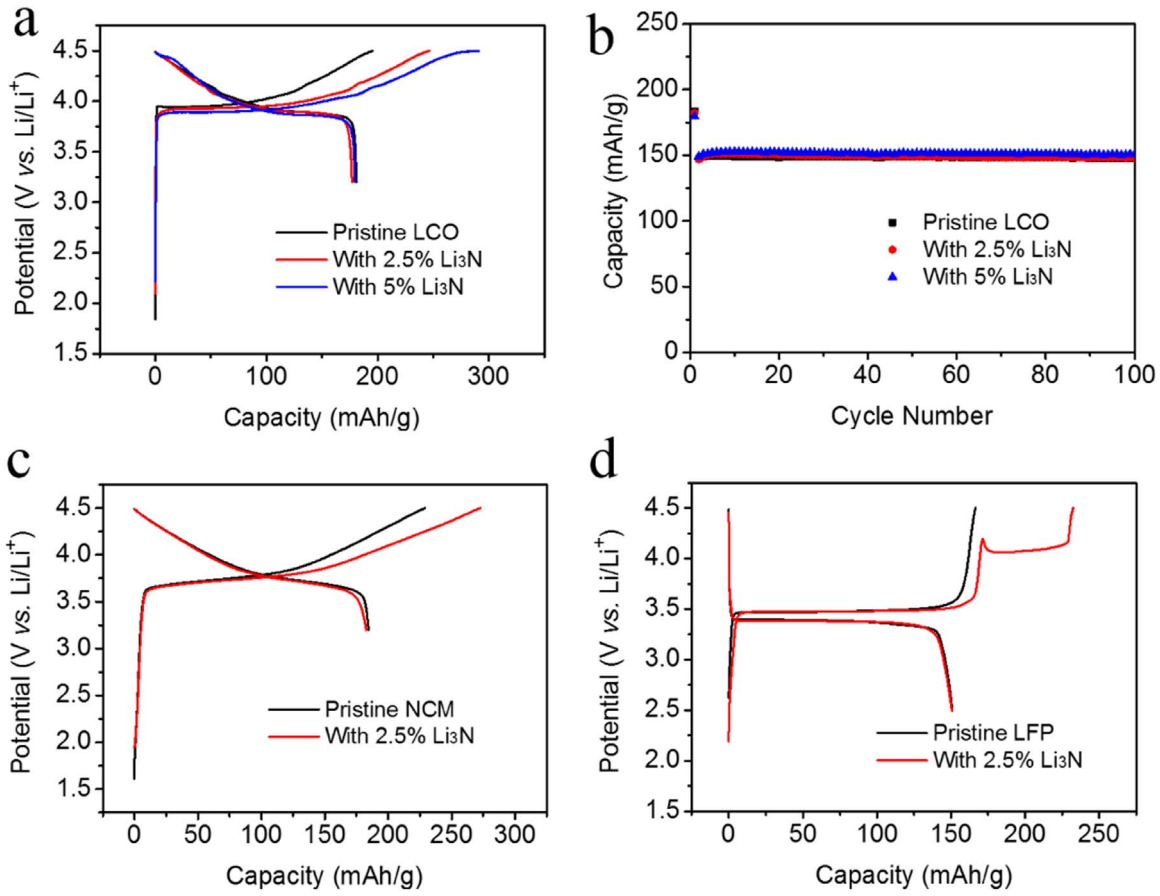

Fig. 4. Electrochemical characteristics of cathodes with Li_3N additive. (a, b) Initial charge and discharge curves (a) and cycling (b) of LCO cathodes with and without the addition of Li_3N. (c) The comparison of initial charge and discharge potential profiles of NCM electrodes with and without the addition of Li_3N. (d) The initial charge and discharge potential profiles of LFP electrodes with and without the Li_3N additive. With the additive of Li_3N, the initial charge capacites of cathodes increase, indicating the lithium "donor" effect of Li_3N. Stable cycling performances are achieved for the LCO electrodes with various amounts of the Li_3N additive. This result shows that the Li_3N additive has negligible negative effect on the stability of the cathode materials.

universal prelithiation material for various cathode materials. High prelithiation efficiency of the Li_3N powder is also achieved for NCM and LFP electrodes. The facile synthesis, high "donor" Li-ion specific capacity, and good stability in battery electrode fabrication processes make the as-prepared Li_3N suitable for potential application in LIBs to offset the first-cycle lithium loss and thus improve the overall battery energy density.

Acknowledgements

Y.C. acknowledges the support from the Assistant Secretary for Energy Efficiency and Renewable Energy, Office of Vehicle Technologies of the U.S. Department of Energy under the Battery Materials Research (BMR) Program. A.P. acknowledges the support from the U.S. Department of Defense through the National Defense Science & Engineering Graduate Fellowship (NDSEG) Program and from Stanford University through the Stanford Graduate Fellowship (SGF) Program.

Appendix A. Supplementary material

Supplementary data associated with this article can be found in the online version at http://dx.doi.org/10.1016/j.ensm.2016.10.004.

References

[1] M.S. Whittingham, Lithium batteries and cathode materials, Chem. Rev. 104 (2004) 4271–4302.
[2] P.G. Bruce, S.A. Freunberger, L.J. Hardwick, J.-M. Tarascon, Li-O_2 and Li-S batteries with high energy storage, Nat. Mater. 11 (2012) 19–29.
[3] B. Dunn, H. Kamath, J.-M. Tarascon, Electrical energy storage for the grid: a battery of choices, Science 334 (2011) 928–935.
[4] B. Scrosati, J. Garche, Lithium batteries: status, prospects and future, J. Power Sources 195 (2010) 2419–2430.
[5] P.G. Bruce, B. Scrosati, J.-M. Tarascon, Nanomaterials for rechargeable lithium batteries, Angew. Chem. Int. Ed. 47 (2008) 2930–2946.
[6] N. Nitta, F.X. Wu, J.T. Lee, G. Yushin, Li-ion battery materials: present and future, Mater. Today 18 (2015) 252–264.
[7] J.M. Tarascon, M. Armand, Issues and challenges facing rechargeable lithium batteries, Nature 414 (2001) 359–367.
[8] C.K. Chan, H.L. Peng, G. Liu, K. McIlwrath, X.F. Zhang, R.A. Huggins, Y. Cui, High-performance lithium battery anodes using silicon nanowires, Nat. Nanotechnol. 3 (2008) 31–35.
[9] H. Wu, Y. Cui, Designing nanostructured Si anodes for high energy lithium ion batteries, Nano Today 7 (2012) 414–429.
[10] P. Verma, P. Maire, P. Novák, A review of the features and analyses of the solid electrolyte interphase in Li-ion batteries, Electrochim. Acta 55 (2010) 6332–6341.
[11] D. Aurbach, Y. Ein-Eli, B. Markovsky, A. Zaban, S. Luski, Y. Carmeli, H. Yamin, The study of electrolyte solutions based on ethylene and diethyl carbonates for rechargeable Li batteries: II. Graphite electrodes, J. Electrochem. Soc. 142 (1995) 2882–2890.
[12] M. Arakawa, J.-I. Yamaki, The cathodic decomposition of propylene carbonate in lithium batteries, J. Electroanal. Chem. Interfacial Electrochem. 219 (1987) 273–280.
[13] K. Xu, Electrolytes and interphases in Li-ion batteries and beyond, Chem. Rev. 114 (2014) 11503–11618.
[14] Y. Matsumura, S. Wang, J. Mondori, Mechanism leading to irreversible capacity loss in Li ion rechargeable batteries, J. Electrochem. Soc. 142 (1995) 2914–2918.
[15] C.K. Chan, R. Ruffo, S.S. Hong, Y. Cui, Surface chemistry and morphology of the solid electrolyte interphase on silicon nanowire lithium-ion battery anodes, J. Power Sources 189 (2009) 1132–1140.
[16] J. Hassoun, K.-S. Lee, Y.-K. Sun, B. Scrosati, An advanced lithium ion battery based on high performance electrode materials, J. Am. Chem. Soc. 133 (2011) 3139–3143.
[17] C.R. Jarvis, M.J. Lain, M.V. Yakovleva, Y. Gao, A prelithiated carbon anode for